Journal of Alloys and Compounds 702 (2017) 338–345

Contents lists available at ScienceDirect

Journal of Alloys and Compounds

journal homepage: http://www.elsevier.com/locate/jalcom

Anodisation of AZ91D magnesium alloy in molybdate solution for corrosion protection

A.D. Forero López, I.L. Lehr, S.B. Saidman*

Instituto de Ingeniería Electroquímica y Corrosión (INIEC), Departamento de Ingeniería Química, Universidad Nacional del Sur, Av. Alem 1253, 8000, Bahía Blanca, Argentina

ARTICLE INFO

Article history:
Received 24 May 2016
Received in revised form
9 December 2016
Accepted 3 January 2017
Available online 4 January 2017

Keywords:
Magnesium alloy
Corrosion resistance
Anodisation
Molybdate

ABSTRACT

We report the formation of a protective film on magnesium alloy AZ91D by means of anodisation under potentiostatic conditions in a molybdate solution. Results of the characterisation of the films by scanning electron microscopy (SEM), X-ray diffraction (XRD) and X-ray photoelectron spectroscopy (XPS) are presented. The anodic film is mainly composed by magnesium oxides or hydroxides and molybdenum oxides. The corrosion protection performance of the coating was investigated in Ringer solution by monitoring the open circuit potential, polarisation techniques and electrochemical impedance spectroscopy (EIS). The coated electrodes exhibit significant corrosion protection properties due to the presence of molybdenum species in the film.

1. Introduction

Magnesium alloys are the lightest metallic structural materials, and hence they have widely applications such as in automotive, aerospace and electronic industries. But the alloys are one of the most electrochemically active materials and their poor corrosion resistance is a major impediment to their applications. Moreover, magnesium alloys can be used in biodegradable hard tissue implants because they degrade naturally in the physiological environment [1]. However, in this case the major drawback is also their low corrosion resistance in the body fluids.

Chromates produced the most efficient inhibition of Mg alloys but since Cr(VI) presents both health and environmental hazards, many efforts have been made in finding new protection strategies. Surface treatments such as chemical conversion coatings, anodising and electrochemical plating have been developed [1–3].

Molybdenum is well known as a localised corrosion inhibitor when present in electrolyte as Mo(VI) or as an alloying element in iron-based alloys [4,5]. The use of molybdate in different treatments to protect Mg alloys against corrosion has been the subject of various works [2,6–9]. Molybdate anion has many advantages such as low toxicity and high stability in aqueous media [10,11].

AZ91D is one of the most commonly used magnesium alloys. Its corrosion resistance depends on the presence of impurity elements acting as active cathode and the microstructure [12,13]. The alloy has a two phase microstructure, a matrix of α-grains (magnesium rich) with the β phase (intermetallic $Mg_{17}Al_{12}$) along the α-grain boundaries.

For biomedical applications the amount of Al released from the Mg alloys must be carefully controlled. A high Al concentration is harmful to neurons and osteoblasts and may be a possible cause of dementia and Alzheimer's disease [14,15].

In this work results are presented on the anodisation of AZ91D alloy in the presence of molybdate solutions in order to improve the corrosion resistance of the material. The characterisation of the formed coatings was done using electrochemical measurements including open circuit potential measurements, potentiodynamic polarisation tests and electrochemical impedance spectroscopy (EIS). The films were also analysed by SEM, EDS, XPS and XRD techniques.

2. Material and methods

The working electrodes were prepared from rods of die-cast AZ91D magnesium alloy (composition: 8.978% Al, 0.6172% Zn, 0.2373% Mn, 0.2987% Si, 0.1189% Cu, 0.00256% Ni, 0.0176% Fe, 0.00164% Ca, 0.01154% Zr, remainder Mg). The rods were embedded in a Teflon holder with an exposed area of 0.070 cm^2.

* Corresponding author.
E-mail address: ssaidman@criba.edu.ar (S.B. Saidman).

http://dx.doi.org/10.1016/j.jallcom.2017.01.030
0925-8388/

The microstructure of the alloy was revealed by etching in a Nital solution (97 mL ethanol and 2 mL nitric acid) for 1 min. The SEM micrograph of the etched sample is presented in Fig. 1, where two different zones can be observed. According to literature two main phases should be distinguished: a substitutional solid solution of aluminium in magnesium (α phase) and the intermetallic $Mg_{17}Al_{12}$ (β phase) along the α-grain boundaries [16,17]. EDS spectra of the two zones are also presented in the figure. While a strong Mg peak is present in both spectra, an enhanced Al signal is observed in the spectrum from the light grey zone. The results indicate that the light grey zone corresponds to the Al-reach β phase present in the alloy, which in general is considered more resistant to corrosion than the Mg-rich α phase (darker zone).

Before each experiment, the exposed surfaces were polished to a 1000 grit finish using SiC, then degreased with acetone and washed with triply distilled water. Following this pretreatment, the electrode was immediately transferred to the electrochemical cell. All the potentials were measured against a saturated Ag/AgCl and a platinum sheet was used as a counter electrode. The cell was a 20 cm^3 Metrohm measuring cell.

The electrodes were treated in an electrolyte solution containing sodium molybdate dihydrate ($Na_2MoO_4 \cdot 2H_2O$) (0.05–0.25 M) in a purified nitrogen gas saturated atmosphere. The temperature was maintained at 20 °C. The pH of the solution was adjusted by addition of NaOH. All chemicals were reagent grade and solutions were made in twice distilled water.

Electrochemical measurements were done using a potentiostat-galvanostat PAR Model 273A and VoltaLab40 Potentiostat PGZ301. The frequency used for the impedance measurements was changed from 100 kHz to 10 mHz, and the signal amplitude was 10 mV. A dual stage ISI DS 130 SEM and an EDAX 9600 quantitative energy dispersive X-ray analyser were used to examine the electrode surface. X-ray diffraction analysis was carried out using a Rigaku X-ray diffractometer (model Dmax III-C) with Cu Kα radiation and a graphite monochromator. X-ray photoelectron spectroscopy (XPS) have been measured in a Specs setup operating. The XPS analysis

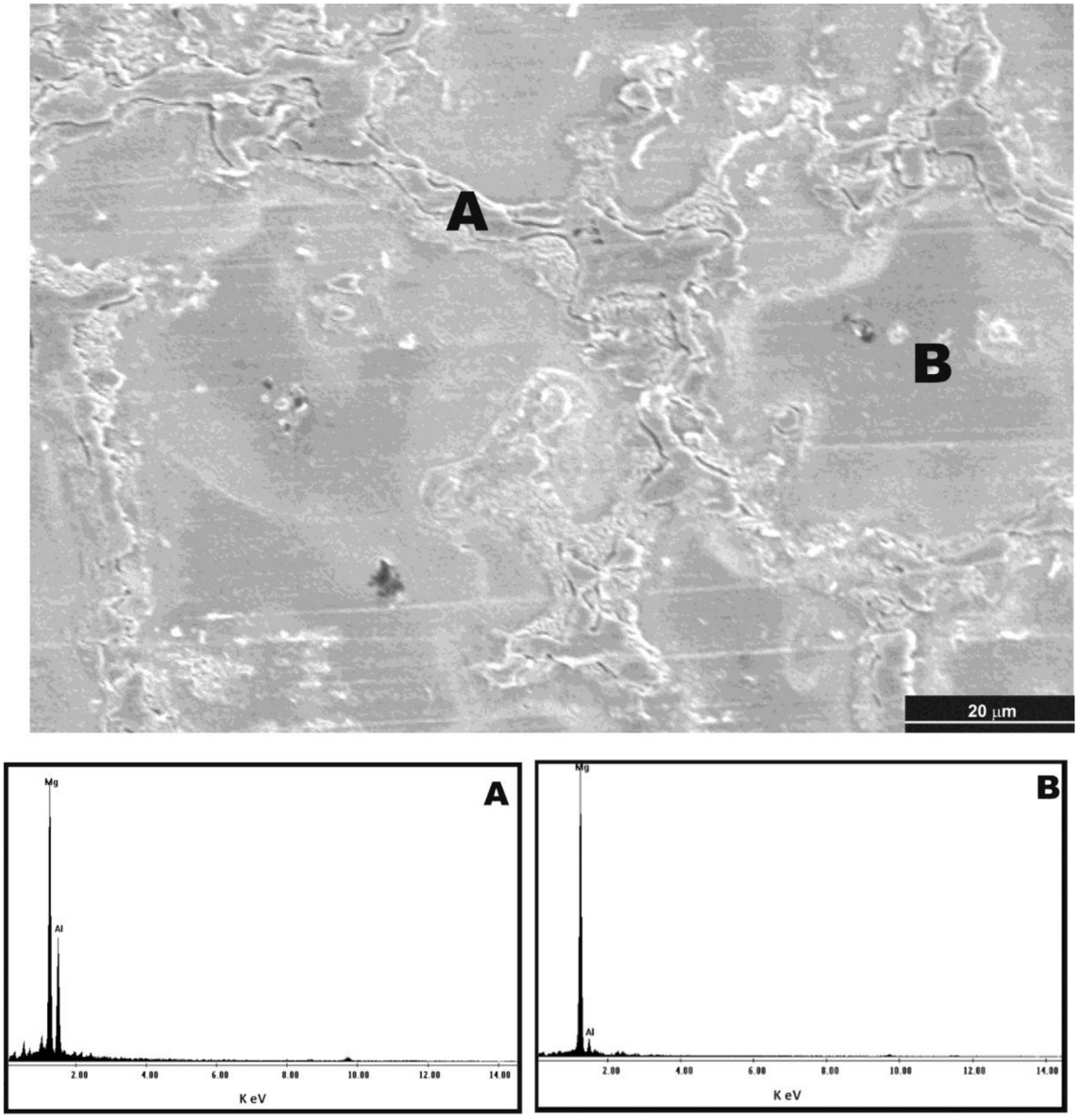

Fig. 1. SEM micrograph of microstructure of die-cast AZ91D alloy. EDS spectra of the α (point A) and β (point B) phases. The microstructure of the alloy was revealed by etching in a Nital solution for 1 min.

chamber is equipped with a dual anode (Al/Mg) X-ray source and a 150 mm hemispherical electron energy analyser (PHOIBOS). The analyser operates in fixed analyser transmission (FAT) mode with pass energy of 30 eV. The energies of all spectra were referenced to the C 1s peak at 285.0 eV. All the XPS spectra were deconvoluted using the CasaXPS software with a Gaussian-Lorentzian mix function.

Film adhesion was tested measuring the force necessary to peel-off the film using a Scotch® MagicTM double coated Tape 810 (3 M) and a Mecmesin basic force gauge (BFG 50 N).

The corrosion performance was investigated in Ringer solution at 37 °C by a potentiodynamic method, by the variation of the open circuit potential (OCP) as a function of time and by electrochemical impedance spectroscopy (EIS). The electrodes were allowed to equilibrate at the fixed voltage before the ac measurements. The composition of Ringer solution is (per 1 L) 8.60 g NaCl, 0.30 g KCl and 0.32 g $CaCl_2 \cdot 2H_2O$.

The Tafel tests were carried out by polarising from cathodic to anodic potentials with respect to the open circuit potential at 0.001 Vs^{-1} in Ringer solution. Estimation of corrosion parameters was realized by the Tafel extrapolation method. The extrapolation of anodic and/or cathodic lines for charge transfer controlled reactions gives the corrosion current density (i_{corr}) at the corrosion potential (E_{corr}). All experiments were conducted after the steady-state E_{corr} was attained, which normally took 1 h after immersion in the solution.

Each set of experiments was repeated two to four times to ensure reproducibility.

3. Results and discussion

3.1. Coating formation

Fig. 2 displays the transient obtained in 0.25 M MoO_4^{2-} pH 9 solution by applying a potential of 1.0 V (curve a). The current decreases continually until a constant value is reached. The electrode was covered by a black film at the end of the polarisation. For simplicity purposes this film is called Mo-coating.

A different response was obtained when an anion such as nitrate was used (Fig. 2, curve b). Current oscillations are observed and the charge density involved is much higher than that obtained with molybdate. Moreover, in this case whitish corrosion products covering an attacked surface of the substrate were observed, indicating a strong oxidation of the alloy. The results pointed out that the black film significantly improves the corrosion resistance of the substrate.

The current measured during the transient increases as the molybdate concentration increases and as the potential is made more positive (Fig. 3). Independently of the molybdate concentration (0.05–0.25 M), electrodeposition time (5–60 min) and applied potential (0.5–1.15 V), the black film was formed on the electrode surface after polarisation.

When the polarisation was made in a 0.25 M MoO_4^{2-} pH 12 solution, a huge amount of O_2 bubbles were formed causing a detachment of some parts of the black film.

3.2. Coating characterisation

A cross-sectional view of the film formed in 0.25 M MoO_4^{2-} pH 9 solution at 1.0 V indicates an average coating thickness of 70 μm (Fig. 4A). A SEM image shows a mud-cracked structure which seems to be related with dehydration of the film after treatment or with vacuum conditions inside the SEM chamber (Fig. 4B). Conversion coatings formed in molybdate-containing baths revealed a similar type of cracks [2,6]. It is expected that the film becomes hydrated again upon exposure to an electrolyte solution, and then the negative effect of the cracks decreased [2]. The presence of Mo in the film is evidenced by EDX spectrum (Fig. 4C).

The coating is very adherent and could be removed only by mechanical polishing. Adhesion of the film increases as the polarisation time increases, as can be seen from the results shown in Table 1. A film with poorer adhesion was obtained when lower molybdate concentrations were used during anodisation.

The treated and untreated sample were analysed by XRD (Fig. 5). By comparing the XRD patterns of both samples it can be concluded that the anodised sample presents diffraction peaks corresponding

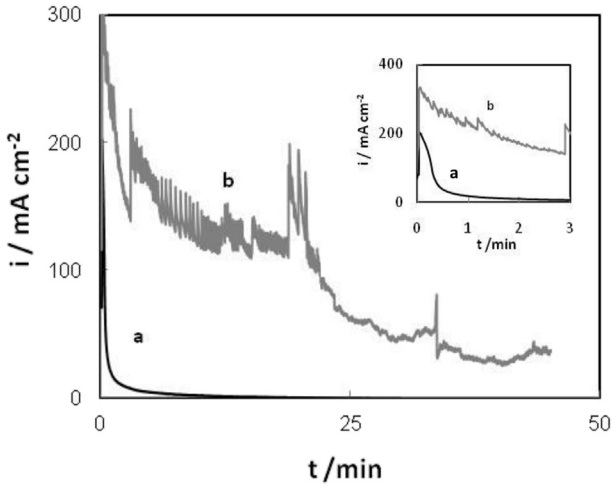

Fig. 2. Potentiostatic transients obtained for AZ91D magnesium alloy at 1.0 V for 45 min in: (a) 0.25 M MoO_4^{2-} pH 9 and (b) 0.25 M NO_3^-, pH 9 solution.

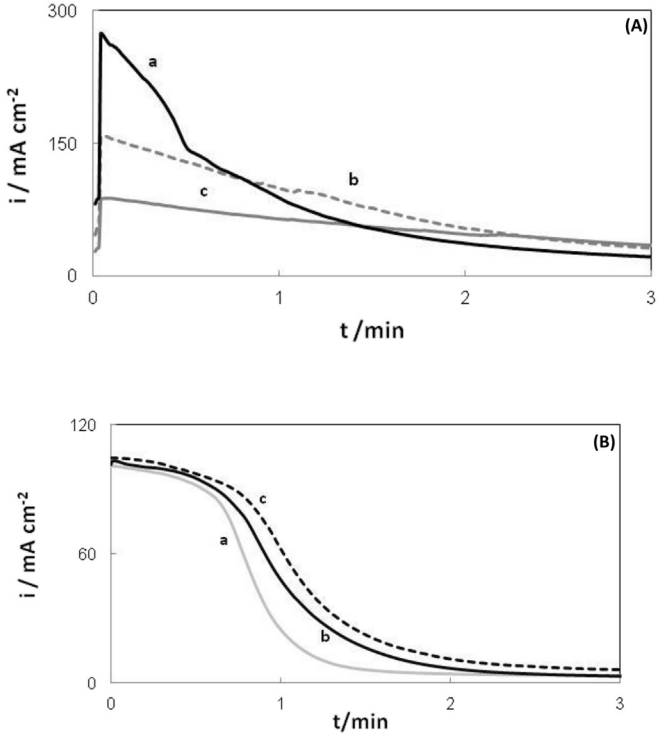

Fig. 3. Potentiostatic transients obtained: **(A)** at 1.0 V for 5 min in x M Na_2MoO_4, pH 9 solution: (a) x = 0.05 M, (b) x = 0.10 M and (c) x = 0.25 M; **(B)** in 0.25 M Na_2MoO_4, pH 9 solution for 5 min by applying a potential of: (a) 0.05 V, (b) 1.0 V and (c) 1.15 V.

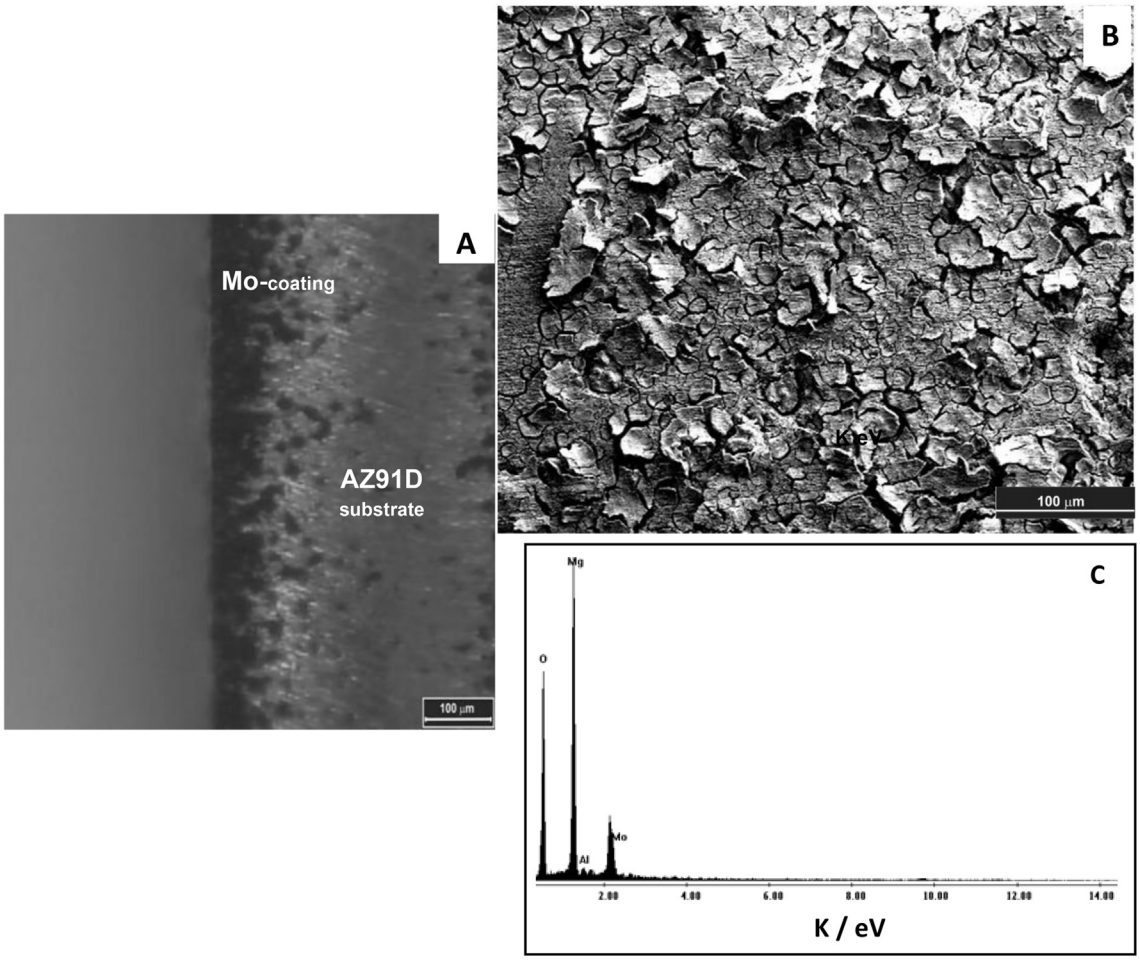

Fig. 4. Cross-sectional image (A), SEM micrograph (B) and EDS spectrum (C) of the Mo-coating formed on AZ91D alloy. The coating was electrosynthesised in a 0.25 M Na_2MoO_4, pH 9 solution at 1.0 V during 45 min.

Table 1
Adherence force obtained for different Mo-coatings after peel-off testing. The coatings were electrosynthesised at 1.0 V. The polarisation time and molybdate concentration employed during anodisation are indicated between parentheses.

Coating	Adherence force/N
Mo-coating (5 min, 0.25 M)	26.00
Mo-coating (15 min, 0.25 M)	23.40
Mo-coating (30 min, 0.25 M)	42.65
Mo-coating (45 min, 0.25 M)	48.55
Mo-coating (45 min, 0.05 M)	35.45

to the substrate. Peaks of MoO_2 are also observed. There are no peaks corresponding to MoO_3 although the presence of amorphous MoO_3 should not be ruled out [18,19].

The chemical composition of the coating was analysed by XPS. The XPS results are shown in Fig. 6. Magnesium, oxygen, molybdenum and aluminum were detected as the major elements. A more detailed XPS analysis of the specific electron binding energies of Mg, O, Mo and Al elements is presented (Fig. 7). The Mg 2p spectrum is displayed in Fig. 7A indicating that Mg in the coating is present as MgO and $Mg(OH)_2$ [2,8,20]. The spectrum of O 1s is presented in Fig. 7B. The peak at 531.25 eV is attributed to metal oxides, MgO and Al_2O_3 [2,8,20]. The binding energies at 232.44 eV and 235.57 eV correspond to Mo(VI) state in molybdenum trioxide (in the form of MoO_3. H_2O) [2] and the peaks at 231.52 and

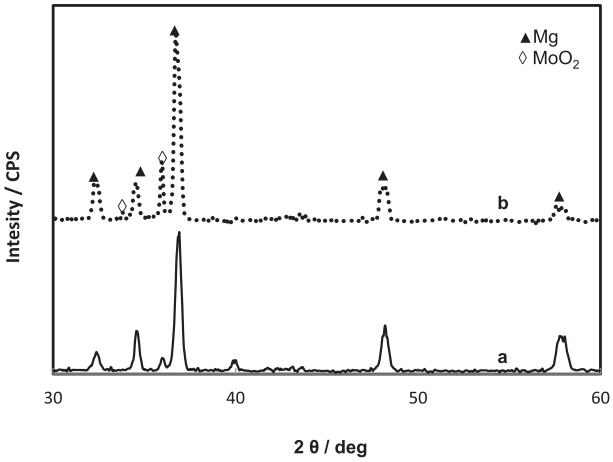

Fig. 5. XRD spectra for: (a) AZ91D alloy and (b) Mo-coating formed on AZ91D alloy. The film was electrosynthesised in 0.25 M Na_2MoO_4, pH 9 solution at 1.0 V during 45 min.

234.72 eV are attributed to the Mo(IV) state in molybdenum dioxide (in the form $MoO(OH)_2$ and MoO_2) [2] (Fig. 7C). The ratio between Mo(VI) and Mo(IV) was 0.794. The signal at 74.8 eV in the Al 2p spectrum (Fig. 7D) is assigned to Al_2O_3 according to literature

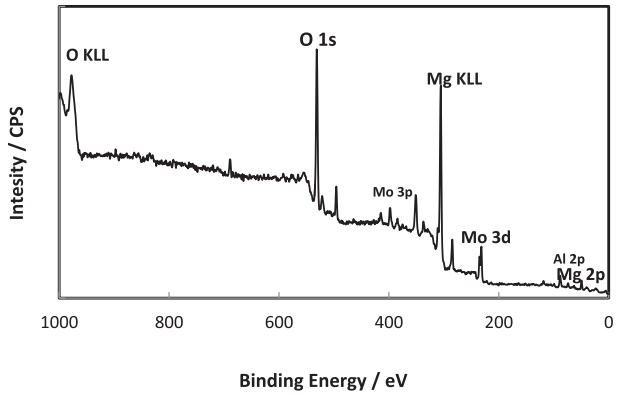

Fig. 6. XPS survey spectrum of Mo-coating formed on AZ91D alloy. The film was electrosynthesised in 0.25 M Na_2MoO_4, pH 9 solution at 1.0 V during 45 min.

data [8,21]. Based on the XPS result, it was concluded that the molybdenum coating was mainly composed of magnesium oxides or hydroxides, aluminium oxide and molybdenum oxides.

The results presented in this work indicate that molybdenum species are incorporated into the film formed at 1 V. Both Mo(VI) and Mo(IV) compounds have been detected in the coating. Moreover, MoO_3 is a white compound and the observed black color of the samples indicates the presence of MoO_2. The obtained results are in accordance with literature data. It was reported the formation of a black film on Mg-Zn-Y-Zr alloy when the material was immersed in a molybdate/phosphate bath [7]. The black color was attributed to the presence of MoO_2. Both oxides, MoO_2 and MoO_3, were detected in a film formed on AZ31 by chemical conversion from a molybdate/phosphate/fluorinate aqueous solution [8] and also in a coating deposited on AZ91D alloy from a solution containing molybdate and cerium nitrate [2].

It is known that the chemistry of molybdenum is very complex. The metal can form a wide variety of stoichiometric and non-stoichiometric oxides. The nature and composition of the surface oxides vary depending on the nature of the medium, electrolyte pH and electrode potential [22]. It was proposed that a partial oxidation of substoichiometric Mo_xO_{3x-1} toward Mo(VI) species at the utmost surface occurs [19]. Considering the Pourbaix diagram of Mo, under the experimental conditions applied in this work the stable species should be Mo(VI). But MoO_2 was found to be the main oxide formed on molybdenum at potentials between 0.5 and 2.0 V in acid solutions [23]. This oxide was also found in the film formed in alkaline solutions at high positive potentials [24,25].

3.3. Anticorrosion properties of the coating

Fig. 8A displays the OCP of AZ91D alloy with and without the coating in Ringer solution as a function of time. As seen, the

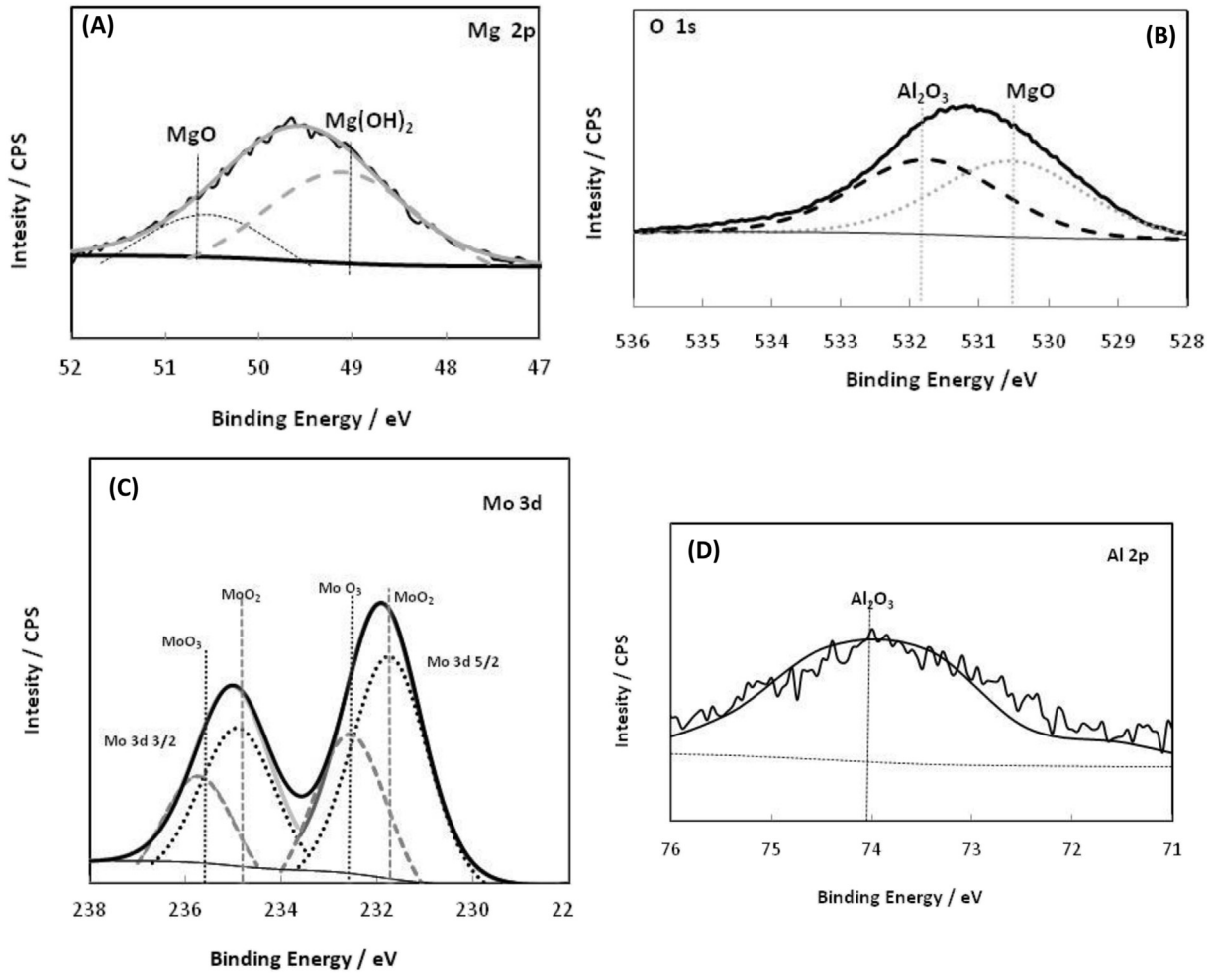

Fig. 7. XPS intensities of: (A) Mg 2p, (B) O 1s, (C) Mo 3d and (D) Al 2p. The film was electrosynthesised in 0.25 M Na_2MoO_4, pH 9 solution at 1.0 V during 45 min.

potential of the coated electrode has a tendency to move toward more negative values with increasing immersion time. But this OCP value is higher than that of the bare alloy even after 40 h of immersion, suggesting that the film is an effective protective coating. The coating remained practically intact after immersion in Ringer solution for 12 h (Fig. 8B).

After the OCP measurements, the electrolyte solutions were analysed to determine the concentration of released ions from the samples (Table 2). The results corroborate that the presence of the coating substantially decreases the corrosion of the substrate.

Fig. 9 shows the Tafel polarisation curves of the film-coated and uncoated alloy after immersion in Ringer solution. Estimation of corrosion parameters (E_{corr}), cathodic (B_c) and anodic (B_a) Tafel slopes and corrosion current (i_{corr}) is shown in Table 3. As can be seen, the presence of the coating causes an anodic shift of the E_{corr} and a one order of magnitude decrease in the corrosion current density.

The degree of protection imparted by the coating can also be evaluated by comparing potentiodynamic polarisation curves in Ringer solution (Fig. 10A). The bare alloy shows no passivation state and the current density increases at - 1.43 V. On the contrary, the curve corresponding to the sample polarised at 1.0 V during 45 min shows a small current density (in the order of 1 μA cm^{-2}) until pitting corrosion initiates at - 0.70 V. It can be also observed in the same figure that when the polarisation time in molybdate solution diminishes the onset of current increase shifts towards more negative potentials. The same tendency was found when lower molybdate concentrations were used during film formation (Fig. 10B).

In order to confirm the corrosion inhibitory effects of MoO_4^{2-}, polarisation curves were also obtained for the bare alloy in Ringer solution containing these anions (not shown here). It was found that a significant increase in current density initiated at - 0.90 V for a concentration of 0.25 M. Thus, molybdate in the solution shifted the pitting potential to the noble direction.

To obtain more information about the anticorrosion protection EIS measurements were performed at the corrosion potential in Ringer solution (Fig. 11). The impedance spectrum of the uncoated sample, as most of the magnesium alloys shows two capacitive loops and one inductive loop [26] (Fig. 11, curve a). It is generally agreed that the polarisation resistance (Rp) corresponds to the diameter of the capacitive loops. A larger R_p value was obtained for the treated sample immersed in the corrosive solution, indicating a corrosion protection. (Fig. 11, curve b). On the other hand, the

Table 2
Elemental analysis corresponding to a Ringer solution after 2 h of immersion of uncoated AZ91D alloy and Mo-coating/AZ91D. The coating was electrosynthesised in 0.25 M Na_2MoO_4, pH 9 solution at 1.0 V during 45 min.

Sample	Al (mg/L)	Mg (mg/L)	Mo (mg/L)
AZ91D	0.42	2.13	–
Mo-coating/AZ91D	0.08	<0.050	<0.050

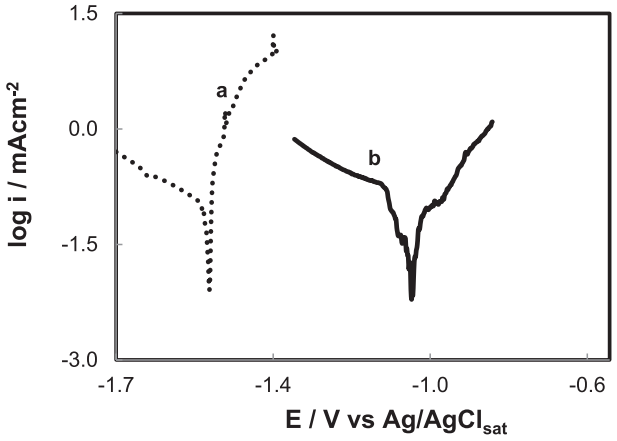

Fig. 9. Tafel curves obtained in Ringer solution at 37 °C for: (a) uncoated AZ91D alloy. and (b) Mo-coating/AZ91D.

Table 3
Corrosion parameters calculated from Tafel polarisation plots for uncoated AZ91D and Mo-coating formed on AZ91D alloy. The mean values and their standard deviation are presented.

	E_{corr}/V	i_{corr}/mAcm^2	B_a/V	B_c/V
AZ91D	−1.501 ± 0.050	0.1050 ± 0.0050	0.045	−0.293
Mo-coating/AZ91D	−1.044 ± 0.020	0.0165 ± 0.0005	0.092	−0.061

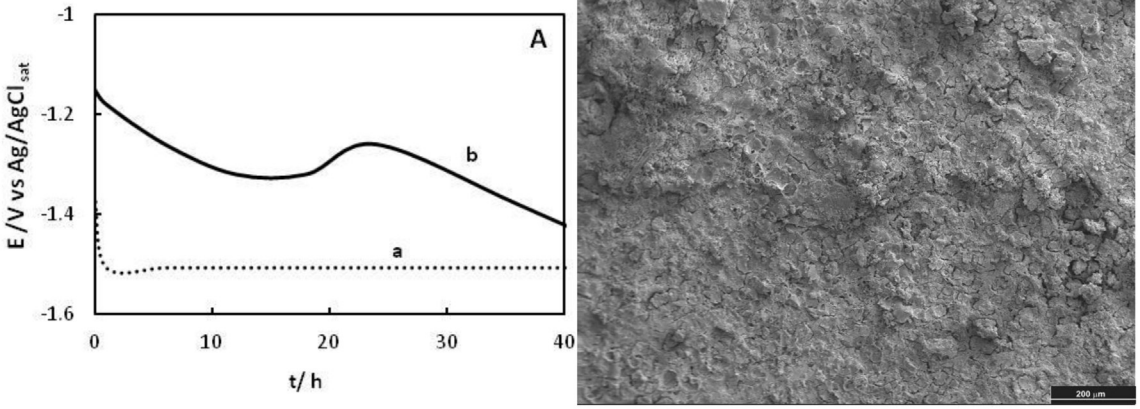

Fig. 8. (A) Time dependence of the OCP in Ringer solution for: (a) AZ91D magnesium alloy and (b) Mo-coating/AZ91D. **(B)** SEM micrograph of Mo-coating formed on AZ91D after 12 h of immersion in Ringer solution. The coating was obtained in 0.25 M Na_2MoO_4, pH 9 solution at 1.0 V during 45 min.

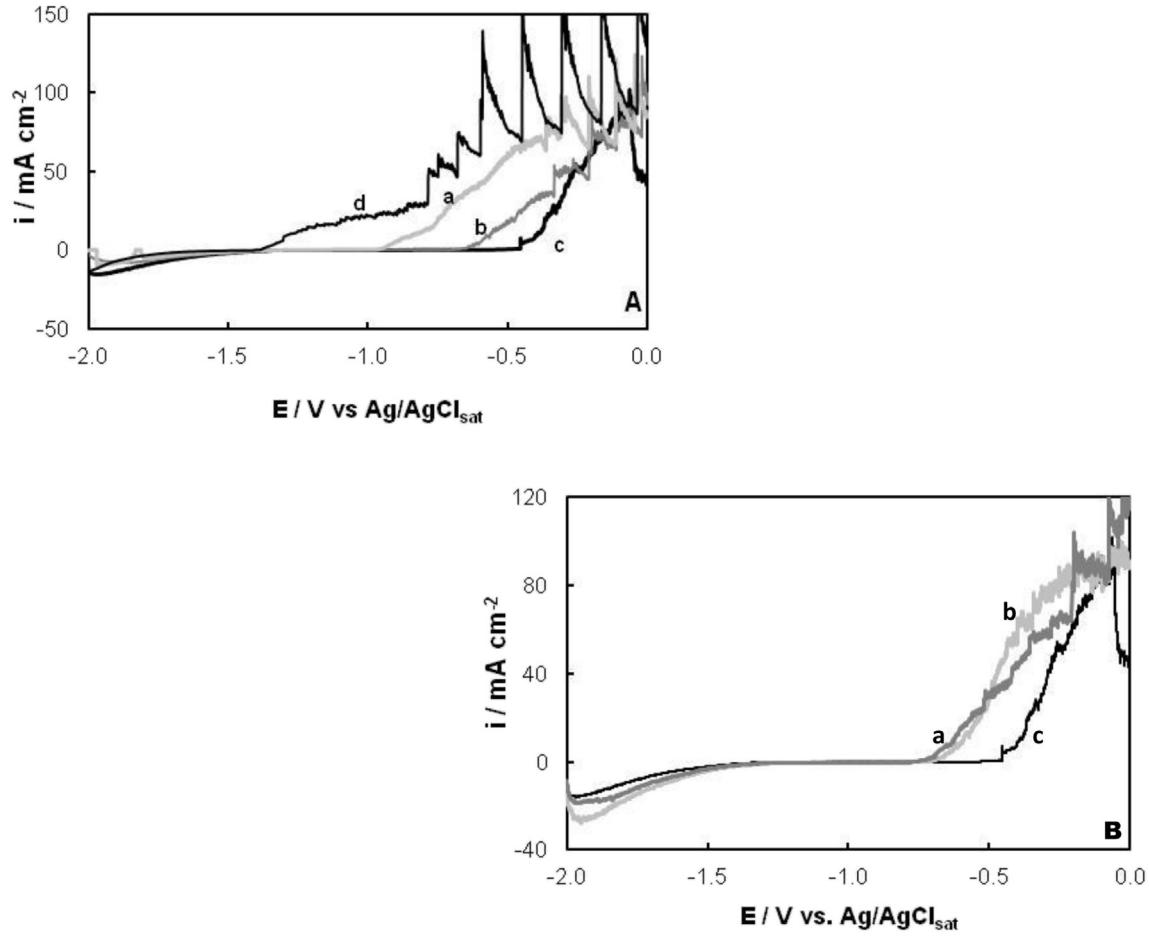

Fig. 10. Polarisation behavior in Ringer solution at 37 °C for Mo-coating/AZ91D. **(A)** The coating was formed in a 0.25 M Na_2MoO_4, pH 9 solution at 1.0 V during: (a) 15 min, (b) 30 and (c) 45 min. For comparison, the curve obtained for uncoated AZ91D alloy is included (curve d). **(B)** The coating was formed at 1.0 V during 45 min in: (a) in 0.05 M Na_2MoO_4, pH 9 solution, (b) in 0.10 M Na_2MoO_4, pH 9 solution and (c) 0.25 M Na_2MoO_4, pH 9 solution. The scan rate was 0.001 Vs^{-1}.

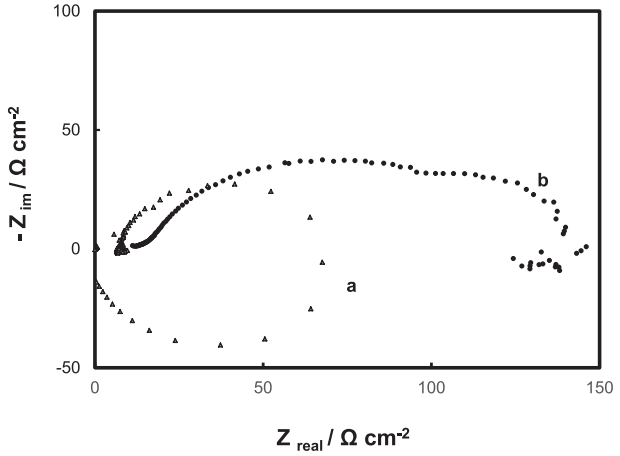

Fig. 11. Nyquist plots of the impedance spectra obtained at the open circuit potential in Ringer solution at 37 °C after 5 min of immersion for: (a) uncoated AZ91D alloy and (b) Mo-coating/AZ91D. The coating was electrosynthesised in 0.25 M Na_2MoO_4, pH 9 solution at 1.0 V during 45 min.

inductive loop at low frequencies is attributed to the relaxation processes of adsorbed species such as $Mg(OH)^+$ or $Mg(OH)_2$ on the electrode surface, which is significant in the absence of a protective layer [27]. A decrease in the size of the inductive loop is related to a weaker interaction between the metal surface and the corrosive solution, indicating again that corrosion is inhibited for the treated sample.

It is postulated that the general corrosion mechanism of Mg alloys involves Mg oxidation to Mg^{2+} with simultaneous water reduction, and the later precipitation of $Mg(OH)_2$ due to the local alkalisation produced by cathodic reactions [28,29]. The α-phase acts as the anode and the β-phase as the cathode.

The AZ91D alloy exhibits a high corrosion rate in Ringer solution. Molybdenum species incorporated in the film are related to the improved corrosion resistance after the anodic treatment. The film not only provide a physical barrier between the substrate and the corrosive medium. Self-healing ability and the inhibition properties of Mo species reduce the dissolution rate of the alloy [9]. The presence of these species into the passive film ensures that protection could be maintained without requiring continuous exposure to the inhibitor solution.

4. Conclusions

A non-toxic coating was obtained on the surface of AZ91D magnesium alloy in a molybdate solution. A relatively simple low-voltage anodising method allows to obtain adherent and uniform films with a thickness of approximately of 70 μm. According to XPS and XRD analyses the coating is probably composed of MgO, $Mg(OH)_2$, Al_2O_3, MoO_3, $MoO(OH)_2$ and MoO_2.

Electrochemical measurements as well as the determination of metal ions concentrations indicated that the coating is able to retard the corrosion of the substrate in Ringer solution. The best results were obtained for anodisation in a 0.25 M MoO_4^{2-}, pH 9 solution at 1.0 V with a polarisation time of 45 min. It was proved that molybdate acts as a pitting corrosion inhibitor for the bare alloy in Ringer solution. Thus the incorporation of molybdenum species in the growing film during anodisation treatment is responsible for the improved corrosion resistance.

Acknowledgements

CONICET (PIP-112-201101-00055), ANPCyT (PICT-2012- 0141) and Universidad Nacional del Sur (PGI 24/M127), Bahía Blanca, Argentina are acknowledged for financial support.

References

[1] H. Hornberger, S. Virtanen, A.R. Boccaccini, Biomedical coatings on magnesium alloys - a review, Acta Biomater. 8 (2012) 2442–2445.
[2] S. Mu, J. Du, H. Jiang, W. Li, Composition analysis and corrosion performance of a Mo-Ce conversion coating on AZ91 magnesium alloy, Surf. Coat. Technol. 254 (2014) 364–370.
[3] J.E. Gray, B. Luan, Protective coatings on magnesium and its alloys a critical review, J. Alloy. Compd. 336 (2002) 88–113.
[4] A. Pardo, M.C. Merino, A.E. Coy, F. Viejo, R. Arrabal, E. Matykina, Pitting corrosion behavior of austenitic stainless steels combining effects of Mn and Mo additions, Corros. Sci. 50 (2008) 1796–1806.
[5] C. Lemaitre, A. Adbel Moneium, R. Djoudjou, B. Baroux, G. Beranger, A statistical study of the role of molybdenum in the pitting resistance of stainless steels, Corros. Sci. 34 (1993) 1913–1922.
[6] J. Hu, Q. Li, X. Zhong, L. Zhang, B. Chen, Composite anticorrosion coatings for AZ91D magnesium alloy with molybdate conversion coating and silicon sol–gel coatings, Prog. Org. Coat. 66 (2009) 199–205.
[7] Y. Song, D. Shan, R. Chen, E.-H. Han, An environmentally friendly molybdate/phosphate black film on Mg–Zn–Y–Zr alloy, Surf. Coat. Technol. 204 (2010) 3182–3187.
[8] T. Ishizaki, Y. Masuda, K. Teshima, Composite film formed on magnesium alloy AZ31 by chemical conversion from molybdate/phosphate/fluorinate aqueous solution toward corrosion protection, Surf. Coat. Technol. 217 (2013) 76–83.
[9] L. Pezzato, K. Brunelli, E. Napolitani, M. Magrini, M. Dabalà, Surface properties of AZ91 magnesium alloy after PEO treatment using molybdate salts and low current densities, Appl. Surf. Sci. 357 (2015) 1031–1039.
[10] X. Li, S. Deng, H. Fu, Sodium molybdate as a corrosion inhibitor for aluminium in H_3PO_4 solution, Corros. Sci. 53 (2011) 2748–2753.
[11] R.W. Kapp Jr., Reference Module in Biomedical Sciences Encyclopedia of Toxicology, third ed., 2014, pp. 383–388.
[12] G. Song, A. Atrens, M. Dargusch, Influence of microstructure on the corrosion of diecast AZ91D, Corros. Sci. 41 (1998) 249–273.
[13] G. Ballerini, U. Bardi, R. Bignucolo, G. Ceraolo, About some corrosion mechanisms of AZ91D magnesium alloy, Corros. Sci. 47 (2005) 2173–2184.
[14] G. Song, Control of biodegradation of biocompatable magnesium alloys, Corros. Sci. 49 (2007) 1696–1701.
[15] Y. Xin, T. Hu, P.K. Chu, In vitro studies of biomedical magnesium alloys in a simulated physiological environment: a review, Acta Biomater. 7 (2011) 1452–1459.
[16] M.C. Turhan, R. Lynch, M.S. Killian, S. Virtanen, Effect of acidic etching and fluoride treatment on corrosion performance in Mg alloy AZ91D (MgAlZn), Electrochim. Acta 55 (2009) 250–257.
[17] G. Song, A. Atrens, X. Wu, B. Zhang, Corrosion behaviour of AZ21, AZ501 and AZ91 in sodium chloride, Corros. Sci. 40 (1998) 1769–1791.
[18] T.M. McEvoy, K.J. Stevenson, Electrochemical preparation of molybdenum trioxide thin films: effect of sintering on electrochromic and electroinsertion properties, Langmuir 19 (2003) 4316–4326.
[19] A. Quintana, A. Varea, M. Guerrero, S. Suriñach, M.D. Baró, J. Sort, E. Pellicer, Structurally and mechanically tunable molybdenum oxide films and patterned submicrometer structures by electrodeposition, Electrochim. Acta 173 (2015) 705–714.
[20] C.D. Wagner, D.E. Bickham, NIST X-ray Photoelectron Spectroscopy Database NIST, 1989.
[21] L. Wang, T. Shinohara, B. Zhang, XPS study of the surface chemistry on AZ31 and AZ91 magnesium alloys in dilute NaCl solution, Appl. Surf. Sci. 256 (2010) 5807–5812.
[22] V.S. Saji, C.W. Lee, Molybdenum, molybdenum oxides, and their electrochemistry, ChemSusChem 5 (2012) 1146–1161.
[23] H. Hixson, P.M.A. Sherwood, Electrochemical oxidation of molybdenum metal in 0.5 M H_2SO_4 studied by core and valence band X-ray photoelectron spectroscopy and interpreted by band structure calculations, Chem. Mater. 8 (1996) 2643–2653.
[24] M.N. Hull, On the anodic dissolution of molybdenum in acidic and alkaline electrolytes, J. Electroanal. Chem. 38 (1972) 143–157.
[25] A.F. Povey, A.A. Metcalfe, The anodic dissolution of molybdenum in alkaline solutions - X-ray photoelectron spectroscopic studies, J. Electroanal. Chem. 84 (1977) 73–81.
[26] A. Srinivasan, C. Blawert, Y. Huang, C.L. Mendis, K.U. Kainer, N. Hort, Corrosion behavior of Mg–Gd–Zn based alloys in aqueous NaCl solution, J. Magnes. Alloy 2 (2014) 245–256.
[27] M. Anik, G. Celikten, Analysis of the electrochemical reaction behavior of alloy AZ91 by EIS technique in H_3PO_4/KOH buffered K_2SO_4 solutions, Corros. Sci. 49 (2007) 1878–1894.
[28] Y. Zhang, Ch. Yan, F. Wang, W. Li, Electrochemical behavior of anodized Mg alloy AZ91D in chloride containing aqueous solution, Corros. Sci. 47 (2005) 2816–2831.
[29] A. Pardo, M.C. Merino, A.E. Coy, R. Arrabal, F. Viejo, E. Matykina, Corrosion behaviour of magnesium/aluminium alloys in 3.5 wt% NaCl, Corros. Sci. 50 (2008) 823–834.